Influence of Corrosion Scales on Steel Corrosion Behavior in CO_2/H_2S Environments

C. I. Ekeocha[1,2*], B. I. Onyeachu[1,3], I. N. Etim[1,4,5], I. N. Uzochukwu[1] and E. E. Oguzie[1,6]

[1]*Africa Centre of Excellence in Future Energies and Electrochemical Systems – Federal University of Technology, Owerri, Imo State, Nigeria*
[2]*Mathematics Programme, National Mathematical Centre, Sheda-Kwali, Abuja, Nigeria*
[3] *Department of Chemistry, Faculty of Science and Computing, Wigwe University Isiokpo, Rivers State, Nigeria*
[4]*Marine Chemistry and Corrosion Research Group, Department of Marine Biology, Akwa-Ibom State University, Nigeria*
[5]*Key Laboratory of Advanced Marine Materials, Key Laboratory of Marine Environmental Corrosion and Bio-fouling, Institute of Oceanology, Chinese Academy of Sciences, Qingdao, China*
[6]*Department of Chemistry, Faculty of Science, Federal University of Technology, Owerri, Imo State, Nigeria*
Corresponding authors: ekeocha.christopher@acefuels-futo.org; emeka.oguzie@futo.edu.ng

Received 18/04/2024; accepted 02/10/2024
https://doi.org/10.4152/pea.2026440305

Abstract
This review overviews recent advancements in studying corrosion scales formed on CS and low alloy steel surfaces in CO_2/H_2S environments. It discusses the chemical reactions, kinetics, mechanisms, classifications, influential factors, formation rates, types, and inhibitive properties of corrosion product scales that develop on steel surfaces. It thoroughly investigates phase transitions, the nature and composition of corrosion product scales, and their impact on the corrosion process by influencing the kinetics of anodic reaction (metal dissolution) and/or cathodic reaction (oxygen reduction/HER), which protect the corroding steel surfaces. Lastly, it emphasizes crucial research areas, knowledge gaps, future perspectives, and approaches for scale mitigation.

Keywords: CO_2/H_2S corrosion; steel corrosion, corrosion mechanisms; corrosion scales; $FeCO_3$; FeS.

Introduction•

CS and low steel alloys are widely used materials in oil and gas industries, for constructing pipelines, drilling rigs, and storage tanks.
Their popularity is due to their cost effectiveness, good mechanical and inherent properties, and satisfactory corrosion resistance [1-4]. However, these materials

•The abbreviations and symbols definition lists are in pages 237-238.

are susceptible to corrosion, especially when exposed to aqueous media containing CO_2/H_2S (Fig. 1), which can compromise them. While dry CO_2/H_2S gas is not considered corrosive, in an aqueous media, it can cause water to act as a catalyst for steel corrosion [5]. Studies in existing literature have suggested that the presence of CO_2 in an oil field can lead to "sweet corrosion", as its dissolution in water produces H_2CO_3, which can accelerate CS corrosion [6-10].

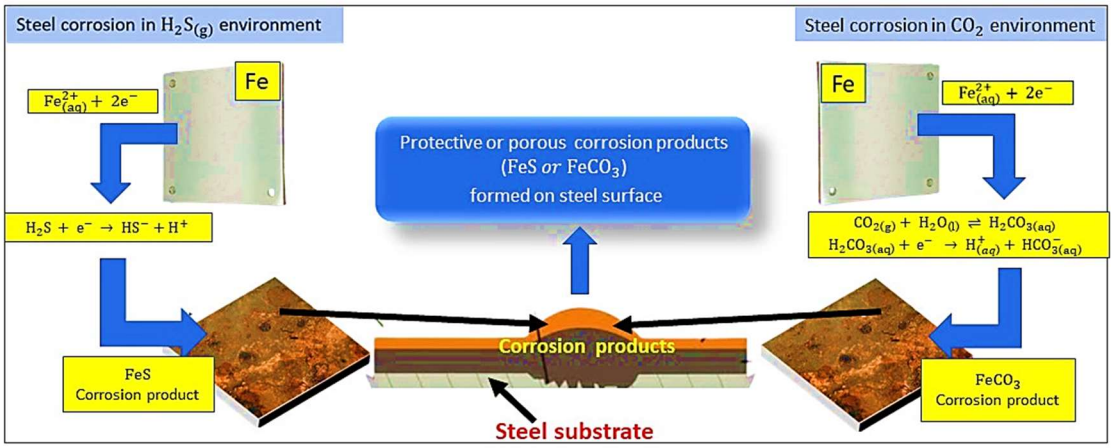

Figure 1: Steel corrosion in H_2S/CO_2 gas environments.

A study conducted in 2002, by the US Federal Highway Administration, found that the annual cost of metal corrosion is approximately $276 billion. This represents 3.1% of the US Gross Domestic Product, 16 times greater than the total cost of weather-related corrosion [11-13]. A related study also found that 33% of equipment failures in the oil and gas industry were due to corrosion, particularly caused by CO_2/H_2S [14-24]. More than half of this percentage is due to fluids causing CO_2, H_2S, or mixed CO_2/H_2S metals dissolution, making it the most widely studied type of corrosion. Several academic studies have been conducted to explore the effects of H_2S [25-31], CO_2 [32-41], and CO_2/H_2S mixed corrosion [42-51] on different grades of low-alloy steels in varying environmental conditions.

The influence of CO_3^{2-} deposit's physical properties on CS local corrosion was investigated by [52]. The study found that the presence of corrosion deposits ($FeCO_3$) regulates the CR of steel through anodic mass transport to and from its surface rather than through cathodic HER. It also found that corrosion product deposits formed by CO_2 corrosion were often porous and exhibited uneven development, facilitating the penetration of corrosive agents into the steel surface where localized corrosion would occur [52]. Similar studies have investigated localized CO_2 corrosion of CS, closely examining CO_3^{2-} deposit's physical properties, suggesting that, in a mixed reaction system containing CO_2/H_2S, corrosion is primarily controlled by CO_2, leading to the development of $FeCO_3$ corrosion product deposits results when partial pressure ratio of H_2S/CO_2 exceeds 500. Conversely, when H_2S/CO_2 partial pressure is less than 20, H_2S controls CR and leads to the formation of FeS corrosion product deposits [53-55]. A summary of corrosion studies conducted in this area over the last decade is shown in Fig. 2.

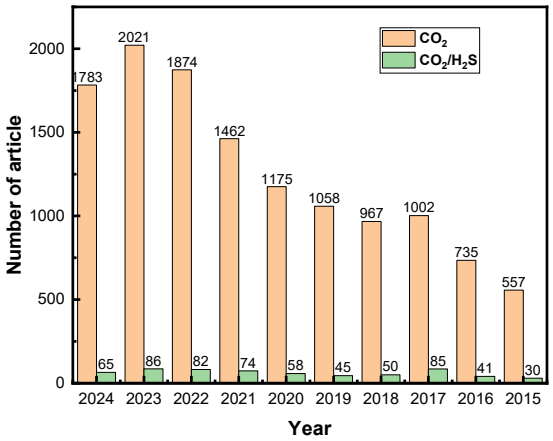

Figure 2: Graphical representation of the corrosion studies in CO_2/H_2S environments over the past decade.

The combination of CO_2 and H_2O in production water used in oil wells to improve production can lead to the formation of H_2CO_3 and trigger electrochemical reactions that cause steel dissolution and the development of corrosion product deposits [56-58], which was found to play an essential role in the kinetics and mechanism of this phenomenon. Thus, extensive research has been conducted to study shape, kinetics, formation mechanisms, predictive models, phase transitions, and influence of corrosion deposits formed in CO_2/H_2S environments on steel CR and their interactions with corrosion inhibitors [59-70].

Although corrosion scales play a crucial role in corrosion science, particularly in protecting CS and low alloy steels during CO_2/H_2S corrosion, there is no review of the literature covering this area. Thus, it becomes imperative that this knowledge gap be filled, for providing a deeper understanding of the corrosion behavior of pre-corroding alloy steels. A schematic representation of the entire review process is shown in Fig. 3.

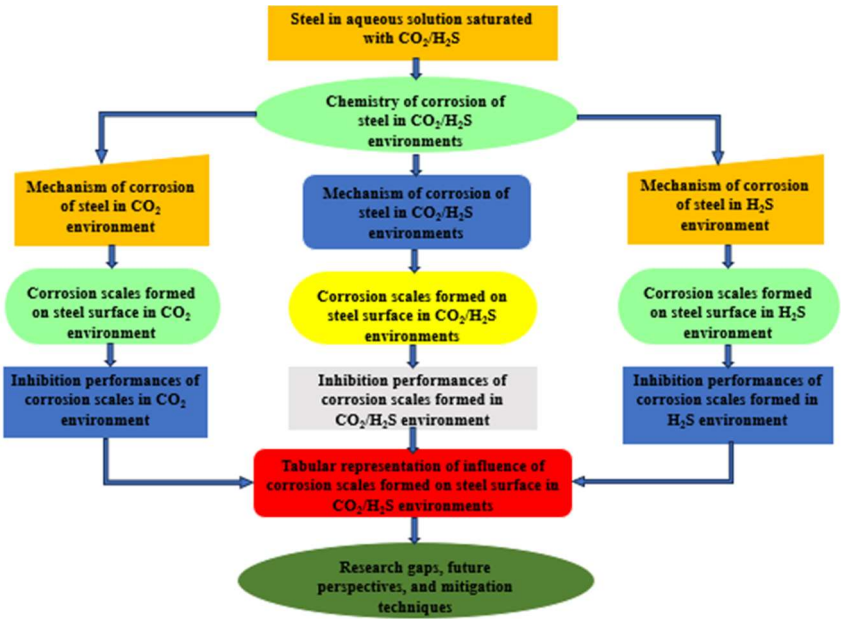

Figure 3: Schematic representation of the entire review process.

Chemistry of corrosion

The phenomenon of corrosion arises from the electrochemical reaction between metals and environmental elements. Essentially, the metal dissolves at the anode, while oxidants are reduced, or hydrogen is produced at the cathode, all in the presence of an aqueous solution. The electrochemical reactions that bring about corrosion are summarized in Eqs. (1-3).

$$M_M M^{2+}_{(aq)} + 2e^-_M \text{ (Metal dissolution/oxidation)} \quad (1)$$

$$2Ox_{(aq)} + 2e_M \rightarrow 2Red(e^-_{redox})_{(aq)} \text{ (Reduction of oxidants)} \quad (2)$$

$$M_M + 2Ox_{(aq)} \rightarrow M^{2+}_{(aq)} + 2Red(e^-_{redox})_{(aq)} \text{ (redox reaction)} \quad (3)$$

Mechanism of steel corrosion in CO_2 environment

The oil and gas industry often experiences CO_2 corrosion, a frequent phenomenon that can occur in various phases of oilfield operations, including production, refining, transportation, and storage of petroleum and its byproducts. The term "corrosion" was originally introduced by American Petroleum Institute, in 1925, but it was not until the early 1940s that CO_2 corrosion was first observed and reported in industry, in Texas, USA [71-73]. CO_2 is commonly found in oil and gas wells conveyed liquids. Research has shown that dry CO_2 is non-corrosive and does not pose the same risk as aqueous H_2S [74]. However, when CO_2 combines with water to form H_2CO_3, it can become corrosive. Nevertheless, it has also been reported that the absence of water in the system can prevent metal dissolution [75]. Studies have been conducted on the corrosion tendency of steel under both supercritical and low partial pressure conditions [76-79].

The presence of wet CO_2 at specific T and pressures can result in severe corrosion problems, particularly in metallic materials built with steel such as storage tanks, pipelines, and flow lines. Metallic corrosion can also lead to equipment failures, fractures in oil tubing, and leakage of products, due to the rupture of pipelines and storage tanks leading to serious safety issues. Consequently, it can affect the productivity and lifespan of the equipment involved in oil and gas production, leading to environmental contamination and financial losses [77].

Existing literature studies have shown that CO_2 is the main cause of oilfield corrosion [78-105]. Unlike mineral acids, CO_2 does not completely dissociate in water, leading to considerable debate as to which dissolved species are involved in the reaction that leads to CO_2 corrosion. T and CO_2 gas partial pressure are important factors that can affect how quickly steel corrodes in a CO_2 atmosphere.

$$CO_{2(g)} + H_2O_{(l)} \rightleftharpoons H_2CO_{3(aq)} \quad (4)$$

There have been numerous discussions in the research literature regarding RDS determination in the reaction between dissolved CO_2 at the cathode and steel surface at the anode, following the equilibrium reaction outlined in Eq. (4). Schwenik has proposed the provision of $[H^+]$ ions from H_2CO_3, resulting in HER (Eq. 5). This hypothesis was followed up by [106], which have postulated the direct reduction of H_2CO_3 at the steel surface, as outlined in Eqs. (6 and 7). They

also have reported on the direct reduction of HCO_3^- ion (Eqs. (8 and 9)) at the cathodic region of the electrochemical reaction. Possible RDS in the cathodic region of the electrochemical reactions leading to corrosion are as follows.

$$\left(HCO_{3(aq)}^-\right): H_{(aq)}^+ + e^- \rightarrow H_{2(g)} \rightarrow H_{2(g)} \quad (5)$$

$$H_2CO_{3(aq)} + e^- \rightarrow H_{(aq)}^+ + HCO_{3(aq)}^- \ (RDS) \quad (6)$$

$$H_{(aq)}^+ + HCO_{3(aq)}^- \rightarrow H_2CO_{3(aq)} \quad \text{and } 2H \rightarrow H_{2(g)} \quad (7)$$

$$HCO_{3(aq)}^- + e^- \rightarrow H_{(aq)}^+ + CO_{3(aq)}^- \ (RDS) \quad (8)$$

$$HCO_{3(aq)}^- + H_{(aq)}^+ + e^- \rightarrow H_{2(g)} + CO_{3(aq)}^{2-} \quad (9)$$

Based on reports from the literature, there is still ongoing debate about specific corrosion processes and the mechanism of reaction involved in them. Numerous elements can influence the speed of steel corrosion, such as partial pressure [107], CO_2/H_2S composition [108-109], corrosion scales morphology, steel microstructure [110], fluid dynamics [111], fluid content influenced by H_2O chemistry (pH, phase ratio, hydrophobicity, and hydrocarbon characteristics) [112-115].

However, numerous reaction mechanisms have been put forth to account for the anodic dissolution of Fe and cathodic reactions (Eqs. (10-13)) in an aqueous CO_2 corrosive system. At pH 6, there are four principal reactions, including an anodic reaction that entails metal dissolution, as well as three cathodic reactions that involve H_2CO_3 and HCO_3^- reduction processes, as demonstrated in Eqs. (11-13), converting H_2CO_3 into HCO_3^-, HCO_3^- into CO_3^{2-} and reducing hydrogen ions to hydrogen gas.

$$\textit{Metal dissolution: } Fe_{(s)} \rightarrow Fe_{(aq)}^{2+} + 2e^- \quad (10)$$

$$2H_2CO_{3(aq)} + 2e^- \rightarrow H_{2(g)} + 2HCO_{3(aq)}^- \quad (11)$$

$$2HCO_{3(aq)}^- + 2e^- \rightarrow H_{2(g)} + CO_{3(aq)}^{2-} \quad (12)$$

$$2H_{(aq)}^+ + 2e^- \rightarrow H_{2(g)} \quad (13)$$

As T increases, corrosion scales like $FeCO_3$, Fe_3C, and/or Fe_3O_4 can develop, providing different degrees of protection to the substrate they cover. Environmental factors also influence the degree of protection provided by corrosion scales. The overall electrochemical reaction is presented in Eq. (14), and this process has been extensively studied and documented [116, 117].

$$CO_{2(g)} + H_2O_{(l)} + Fe_{(s)} \rightarrow FeCO_{3(s)} + H_{2(g)} \quad (14)$$

When CO_3^{2-} and iron ions (Fe) undergo a precipitation reaction, a thin film forms on the metal surface, creating a protective layer of $FeCO_3$ (Eq. 15). The formation of $FeCO_3$ on alloy surfaces is of great importance, due to the protective effect of the corrosion deposit. These deposits play a crucial role in reducing the CR of low alloy steels, by hindering both anodic and cathodic reactions. In addition, corrosion deposits can deter the migration of corrosive agents to the alloy surface, further

reducing the corrosion process. Understanding the properties and behavior of these corrosion scale deposits is important to determine their influence on the CR of metals and alloys. This is especially important when studying the CR of steel in aqueous solutions during CO_2 corrosion. In addition, $FeCO_3$ can easily precipitate in a solution, due to its low solubility at room T (pKsp = 10.54, 25 °C). $FeCO_3$ formation is further illustrated in Eqs. (15-17):

$$Fe^{2+}_{(aq)} + CO^{2-}_{3(aq)} \rightleftharpoons FeCO_{3(s)} \quad (15)$$

$$Fe^{2+}_{(aq)} + 2HCO^{-}_{3(aq)} \rightarrow Fe(HCO_3)_{2(aq)} \quad (16)$$

$$Fe(HCO_3)_{2(aq)} \rightarrow FeCO_{3(s)} + CO_{2(g)} + H_2O_{(l)} \quad (17)$$

Corrosion scale deposits that form on steel surfaces with weak acids can vary in their ability to protect them from further dissolution, depending on specific experimental conditions. Several factors, including pH, contaminants, gases, pressure, T, flow rate, solution chemistry, inhibitor type, and steel metallurgy, can influence the formation and properties of these deposits [118, 119]. During CO_2 dissolution, a $FeCO_3$ layer can form in low-alloy steel (< 9% Cr) and CS.

Mechanism and kinetics of alloy steel corrosion in an H_2S environment

In the oil and gas industry, industrial operations always involve the presence of three significant weak acids (H_2CO_3, CH_3COOH, and H_2SO_4). Numerous literature works have reported that the presence of acids significantly increases the CR of CS and low alloy steels, as evidenced by reports [120-123]. An electrochemical model was proposed by [124] for cathodic reactions in H_2S corrosion, considering a buffering behavior similar to that of CO_2. During this reaction, H_2S contributes with protons to the corroding steel surface via dissociation reactions (Eqs. 18-19).

$$H_2S \rightleftharpoons H^+ + HS^- \quad (18)$$

$$HS^- \rightleftharpoons H^+ + S^{2-} \quad (19)$$

Some researchers have also reported that, like with CO_2, it remains uncertain whether the processes outlined in Eqs. (18 and 19) are in a state of thermodynamic equilibrium. However, it is crucial to consider the chemical kinetics of the reaction, as expressed in Eqs. (20 and 21) [124-126].

$$R_1 = k_1 c_{H_2S} - k_{-1} c_{HS^-} c_{H^+} \quad (20)$$

$$R_2 = k_2 c_{HS^-} - k_{-2} c_{S^{2-}} c_{H^+} \quad (21)$$

where R_2, k_2 and k_{-2} are the respective rates of reactions for forward and backward kinetic constants for HS^- -dissociation reaction.

Although there is limited documentation in the literature on the kinetic rate constants of these reactions, it is generally believed that the dissociation processes of H_2S are faster than those of CO_2. Research studies have extensively investigated the mechanisms of corrosion, particularly focusing on anodic and cathodic reactions that lead to the formation of FeS corrosion deposits on steel surfaces in environments dominated by H_2S. After a thorough review of these reports, a

proposed general mechanism for steel in a wet H_2S environment was presented in Eqs. (22-24), for cathodic and anodic reactions, and in Eq. (25), for the development of corrosion scales [127-131].

$$H_2S + e^- \rightarrow HS^- + H^+ \quad (22)$$

$$HS^- + 2e^- \rightarrow 2S^{2-} + H_2 \quad (23)$$

$$Fe \rightarrow Fe^{2+} + 2e^- \quad (24)$$

$$Fe^{2+} + HS^- \rightarrow FeS + H^+ \quad (25)$$

Existing research studies have shown that the process of H_2S corrosion begins with the gas dissolution in water, resulting in the formation of aqueous H_2S. From there, reactive species (H^+ and HS^-) ions are released through aqueous H_2S dissociation, as dictated by corresponding equilibrium constants in Eqs. (26-28) [131-132]. Dissolution of H_2S in aqueous phase is:

$$H_2S_{(g)} \overset{K_H}{\Leftrightarrow} H_2S_{(aq)} \quad (26)$$

Hydration of aqueous H_2S is:

$$H_2S_{(aq)} + H_2O_{(l)} \overset{K_1}{\Leftrightarrow} HS^-_{(aq)} + H_3O^+_{(aq)} \quad (27)$$

Dissociation of HS^- is:

$$HS^-_{(aq)} \overset{K_2}{\Leftrightarrow} S^{2-}_{(aq)} + H_3O^+_{(aq)} \quad (28)$$

Generally, steel dissolution produces Fe^{2+}, H_2S depolarization releases reactive species, and then the reaction between the metal ion and these reactive species results in FeS corrosion scales (Fig. 4) [133, 134].

Figure 4: Schematic representation of steel corrosion reaction mechanism in an H_2S environment.

Previous literature has shown that H_2S corrosion produces various types of FeS crystal grains, including pyrite, mackinawite (a FeS compound), troilite, and pyrrhotite, which form corrosion scales [135-144].

In general, there is uncertainty regarding the composition and properties of FeS corrosion deposits that initially form on steel surfaces. Nevertheless, some experts have theorized that mackinawite could be the primary corrosion scale, due to its exceptionally rapid formation kinetics at the electrode surface. Using various published sources [145-148], a possible chemical pathway involving Fe in acidic solutions containing H_2S gas is outlined.

$$2H^+_{(ads)} + 2e^- \rightarrow H_{2(g)} \quad (29)$$

$$Fe + H_2O \rightarrow FeOH_{(ads)} + H^+ + e^- \quad (30)$$

$$FeOH_{(ads)} \rightarrow FeOH^+_{(ads)} + e^- \quad RDS \quad (31)$$

$$FeOH^+_{(ads)} + H^+ \Leftrightarrow Fe^{2+} + H_2O \quad (32)$$

Corrosion scales formed on steel in CO_2/H_2S environments

Due to the corrosive and toxic nature of H_2S gas, the oil and gas industry faces numerous issues including that of corrosion. Over the last seven decades, research into the effects of H_2S corrosion on metals used in this sector has increased significantly.

In 1958, [149] discovered mackinawite as the first corrosion deposit to form on a steel surface in an H_2S environment. Over time, corrosion scales can metamorphose into either pyrite and/or pyrrhotite. A separate review of CO_2/H_2S corrosion under oilfield conditions has highlighted the mechanisms of H_2S formation [150]. Despite extensive research, the studies in this area remain more complicated than initially expected. It has also been reported that corrosion scales formed on steel in H_2S media involve not only sulfide (FeS) but also one of the various types of FeS complex species [150].

In addition, it has been reported that Fe dissolution in bulk solutions could exist as any of the complex species of $FeHS^+_{(aq)}$ rather than Fe^{2+}. The morphology and type of FeS corrosion scales formed depends on specific environmental conditions and reaction kinetics, regardless of H_2S, if iron Ct in the environment increases, steel surfaces exposed to it form thin films of mackinawite, provided FeS formation is thermodynamically possible [151-154].

The kinetics of mackinawite formation are rapid and spontaneous compared to other FeS types. A proposed mechanism for steel corrosion in an environment where H_2S predominates is shown in Eqs. (33-36).

$$H_2S + e^- \rightarrow HS^- + H^+ \quad (33)$$

$$HS^- + 2e^- \rightarrow 2S^{2-} + H_2 \quad (34)$$

$$Fe \rightarrow Fe^{2+} + 2e^- \quad (35)$$

$$Fe^{2+} + HS^- \rightarrow FeS + H^+ \quad (36)$$

Similarly, [44] has reported that the rate of formation of corrosion scales depends on the gas Ct in the system. The surface analysis carried out at a molar ratio of the gases (0.5:1 and 1:1) has also shown that the corrosion deposit formed consists of iron and sulfide (Fig. 5c and 5f).

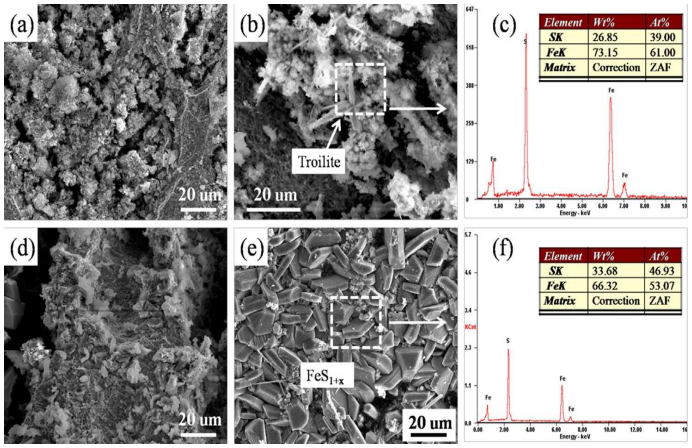

Figure 5: Images of SEM-EDS of pre-corroded X80 steel in an H_2S/CO_2 environment with partial pressure **(a)** 0.5:1 and **(b)** 1:1.

Other types of corrosion deposits formed have also been identified in the study, including troilite and pyrrhotite (Fig. 4). Fig. 6 illustrates H_2S corrosion mechanism.

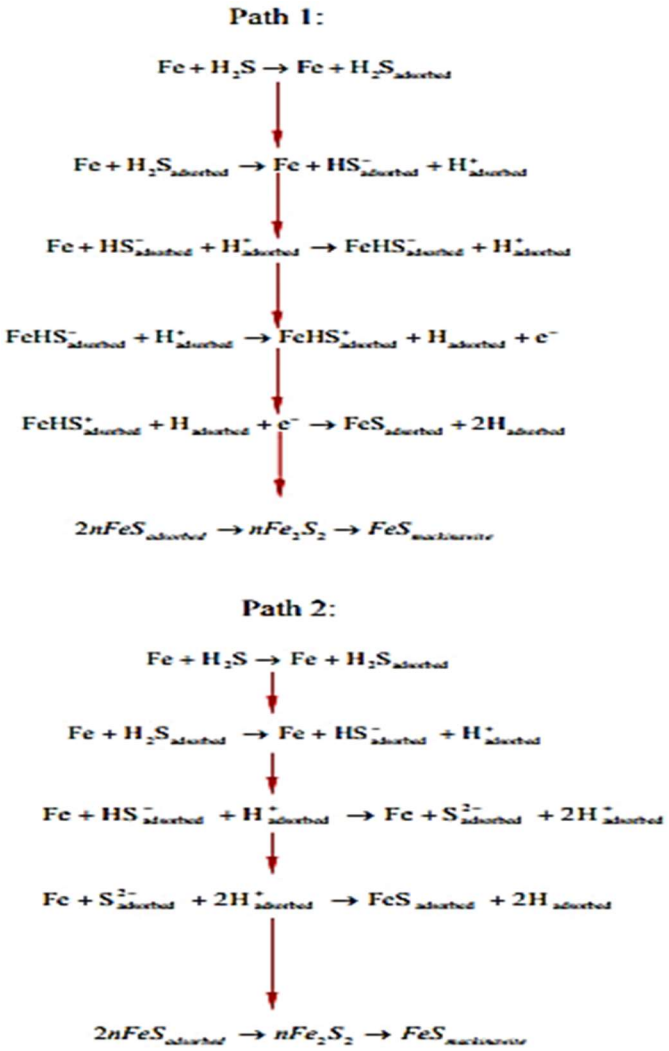

Figure 6: Schematic illustration of H_2S corrosion mechanism.

Corrosion scales formed on steel in CO_2 corrosion.

In an environment containing CO_2/H_2S, corrosion can occur on various types of steel, resulting in the formation of various corrosion scales that deposit on the steel surfaces. The specific nature and characteristics of these corrosion deposits depend on several factors, including the prevailing gas in the system, the partial pressure ratio of the gas, solubility products, IT, T, solution pH, and other relevant conditions. In the 1920s, [155] identified $FeCO_3$, also known as chalybite or siderite, as a type of corrosion scale that forms on steel when exposed to a CO_2-dominant environment. According to [155], precipitated $FeCO_3$ adheres to the steel surface and forms a protective layer of corrosion deposits, which helps mitigate corrosion by reducing the CR through diffusion [156]. Subsequently, precipitation and formation of $FeCO_3$ corrosion deposits on steel have been confirmed by [156], using X-RD analysis. The importance of $FeCO_3$ as a corrosion scale deposit was further highlighted in the early 1970s, when [156] recognized its potential in their widely acclaimed paper on semi-empirical corrosion models, although have not fully considered them. As they have noted, in a CO_2 environment, Fe_3C is another type of corrosion product scale deposit that can form on steel. The type and structure of corrosion deposits that form depend, among other conditions, on the system T. At T below 40 °C, a surface film with an open-porous structure forms on the steel surface, which consists mainly of Fe_3C with a little $FeCO_3$. At T above 60 °C, corrosion deposits consist mainly of external $FeCO_3$ and a few internal porous Fe_3C. However, at T below 60 °C, a dense, protective $FeCO_3$ corrosion layer is formed on the steel surface [156]. Due to the porous nature of inner Fe_3C, its corrosion layer grows on the steel surface as it corrodes and transforms into part of the original steel in a non-oxidized state. Unfortunately, this does not protect the underlying steel from corrosion. [156] have also suggested that $FeCO_3$ may precipitate as $Fe(HCO_3)_2$ or as a $FeCO_3$ hydrate (Eqs. (37-39)), and this topic has been widely discussed in the literature over the years. While most researchers have exclusively used X-RD analysis to assess $FeCO_3$ purity, some have also determined the precipitated solid phase following a solubility experiment [156]. After the discovery of $FeCO_3$ precipitation in CO_2 corrosion by [155], various Fe-related corrosion scales have been identified in several literature studies. These include corrosion scales of $FeCO_3$ [157], Fe_3C [158], Fe_2O_3, and Fe_3O_4 in IOB, as well as FeS and Fe_3O_4 in sulphur-reducing bacteria [159, 160].

$$Fe^{2+}_{(aq)} + CO^{2-}_{3(aq)} \rightarrow FeCO_{3(aq)} \quad (37)$$

$$Fe^{2+}_{(aq)} + 2HCO^{-}_{3(aq)} \rightarrow Fe(HCO_3)_{2(s)} \quad (38)$$

$$Fe(HCO_3)_{2(s)} \rightarrow FeCO_{3(aq)} + CO_{2(g)} + H_2O_{(l)} \quad (39)$$

In their separate studies, [161, 162] have reported $FeCO_3$ decomposition at a high T of 300 ºC, which formed FeO, Fe_2O_3, or Fe_3O_4, stating that the reaction occurred via the path detailed in Eq. (40), in the presence of a small amount of oxygen at high partial pressures of CO_2 and T (t ~ 360 ºC).

$$FeCO_{3(aq)} \rightarrow Fe_3O_{4(s)} + 2CO_{2(g)} + CO_{(g)} \quad (40)$$

Corrosion scales formed on steel in H_2S corrosion.

Research has shown that hydrogen gas environments can lead to greater CO_2 corrosion than that from H_2S in aqueous brines, such as those found in oil fields. In H_2S corrosive environments, steel surfaces tend to form non-stoichiometric polymorphic FeS compounds as the main corrosion product scale [163]. In a research study, pyrrhotite has been also discovered as a major corrosion product scale formed on the surface of 4130 alloys in an environment containing 10% H_2S and argon gas at 204 °C [164].

Types, characteristics and phase changes of corrosion products produced by H_2S

In an aggressive environment containing the corrosive agent, iron(II) monosulphide, also called mackinawite, a metastable species, immediately forms on steel. This process occurs regardless of the corrosive agent (H_2S) Ct in the system, as long as thermodynamics allow FeS formation. In contrast to the slower kinetics of other FeS forms, mackinawite corrosion layer develops quickly on the metal surface. In H_2S environments, various corrosion products scales develop on steel surfaces, including marcasite, cubic FeS, troilite, pyrrhotite, smythite, greigite, pyrite and other compounds [160, 163].

In their study, [164] have suggested that, in an H_2S environment, steel can undergo a series of corrosion product scale reactions with products resulting from $H_2S_{(aq)}$ and $HS^-_{(aq)}$ dissolution and subsequent hydration through chemisorption. Subsequently, this can lead to $FeHS^+_{(aq)}$ formation on the steel surface, which can then be integrated into the rising mackinawite layer through a solid-state reaction. This means that the reaction also takes place in an unsaturated solution, since the formation of the corrosion deposit does not depend on Fe^{2+} Ct or on the corrosive agent (H_2S) solubility. This is due to the faster kinetics of mackinawite formation compared to its dissolution and the diffusion rate of $FeHS^+_{(aq)}$ away from the steel surface during mackinawite dissolution. In addition to the proposed solid-state reaction mechanism between corrosive H_2S and steel. [139] have also provided data to support the reaction mechanism between H_2S and the steel surface, as previously suggested by [151, 152]. The authors have also suggested that $FeHS^+_{(aq)}$ species is always released first, contributing to the growth of other corrosion deposits or nucleates to form mackinawite.

Corrosion scales formed in a mixed CO_2/H_2S corrosion environment

Based on literature studies, mackinawite appears to be the most common corrosion scale occurring in CO_2/H_2S corrosion on steel surfaces. However, there have been cases where $FeCO_3$ scales have been observed alongside mackinawite [64], as shown in Fig. 7. Further studies have also indicated that $FeCO_3$ does not usually integrate the surface morphology of corroded CS. Therefore, it is reasonable to assume in such cases that mackinawite corrosion scale is the main product that forms on steel surfaces, protecting them from further anodic dissolution and exposure to corrosive solutions. Mackinawite corrosion product scale deposits begin to form on the CS surface, hindering the growth of $FeCO_3$ crystals on steel.

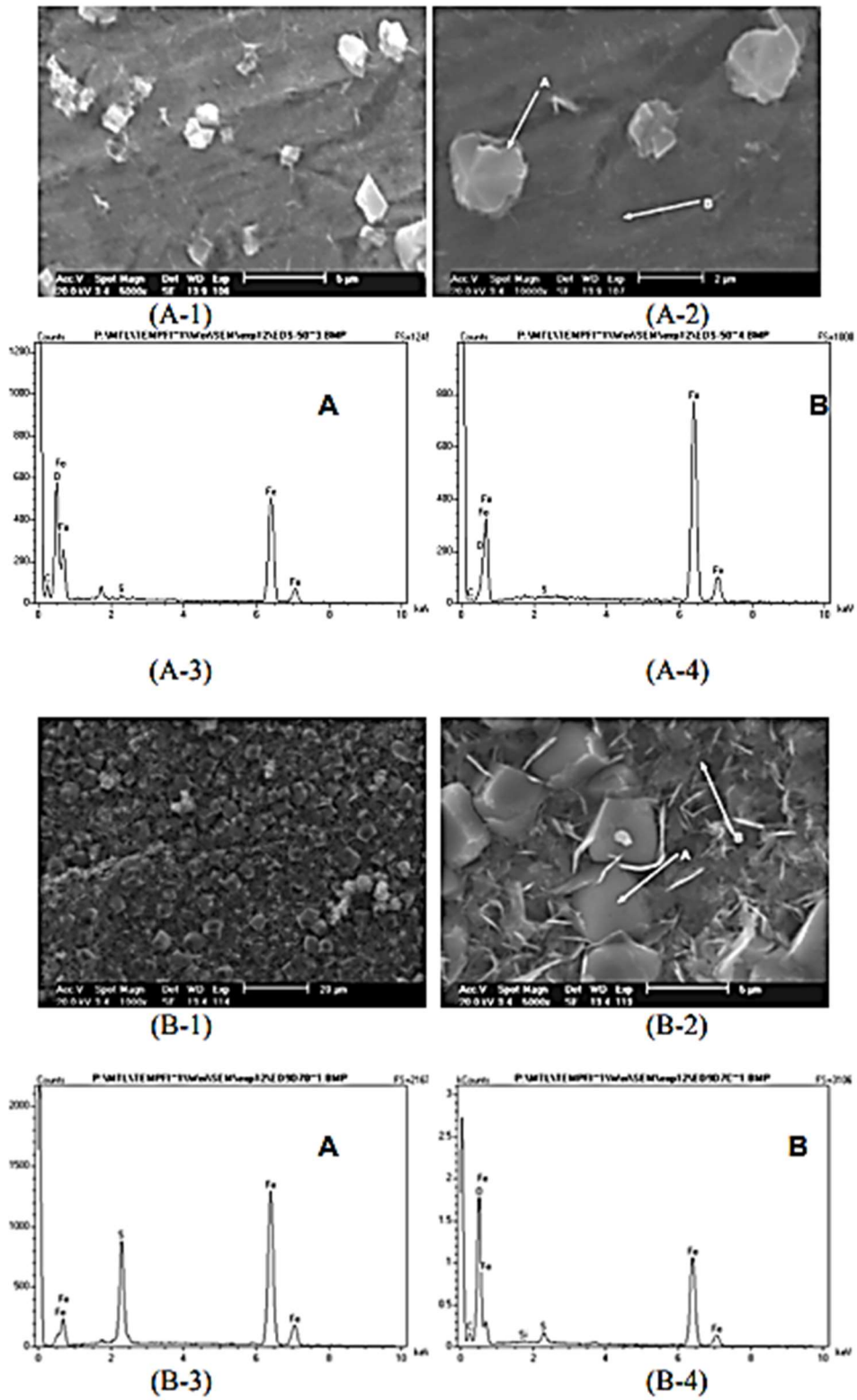

Figure 7: Morphology of corrosion scales formed on X65 CS, with 0.1% H_2S (H_2S/CO_2 gas), pH of 6.6, 80 ℃, 0 and 50 ppm Fe^{2+}, IT of **(A)** 1 and **(B)** 24 h.

X-RD testing on X65 CS has been further conducted by [62], with 0.1, 1, and 10%, H_2S/CO_2 gas, pH of 6.6, 80 ºC and 50 ppm Fe^{2+}, for 24 h. Their findings (Figs. 8 and 9) have revealed that the primary corrosion scale formed on the steel surface

was mackinawite. Interestingly, at a low volume of 0.1% H_2S, mackinawite, and $FeCO_3$ corrosion scales were formed together, while at 1 and 10% H_2S, only the former was created.

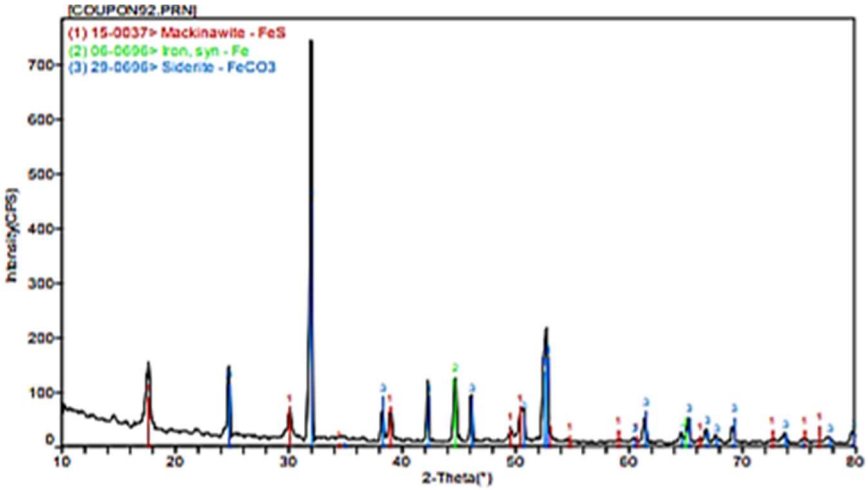

Figure 8: X-RD data for corrosion scales development on the X65 CS surface with 0.1% H_2S (H_2S/CO_2 gas), pH 6.6, 80 ºC, and 50 ppm Fe^{2+}, for 24 h.

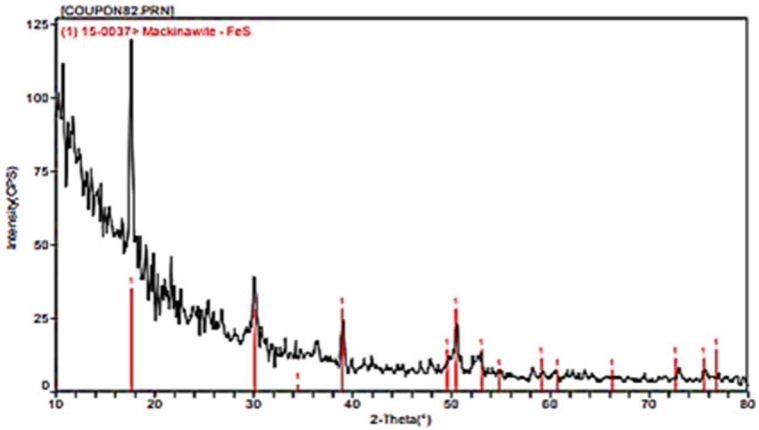

Figure 9: X-RD results of corrosion scales developed on the X65 CS surface at 0.1% H_2S (H_2S/CO_2), pH 6.6, 80 ºC, and 50 ppm Fe^{2+}, for 24 h.

Inhibitive performances of corrosion scales for steel in H_2S corrosion

MS and low alloy steels tend to develop various corrosion scale deposits on their surfaces when exposed to an aqueous environment containing H_2S. At an early stage, Fe_9S_8 is initially formed as a thin layer on the steel surface. Some notable authors have reported that corrosion scales can reduce CR by forming a protective barrier layer on the steel surface, which impedes the penetration of corrosive species. However, as the Fe_9S_8 layer becomes thicker over time and starts fracturing, CR increases. Also, more corrosion scales such as pyrite and pyrrhotite gradually form on steel, which further increases CR [162, 163].

In a related study, [61] investigated the effect of H_2S on Fe corrosion, at pH from 3 to 5, IT of 2 h, and Ct of 0.04 mmol/dm^{-3}. They have observed that E_{corr} of Fe decreased from an initial value of -613 mV to a relatively stable value of -653 mV, within 5 min

IT, at a pH of 3, in an H_2S-free acidic solution (0.5 mmol/dm^{-3} H_2SO_4 over Na_2SO_4), which was the blank. With a higher H_2S Ct of 0.02 and 0.05 mmol/dm^{-3} in a similar solution, E_{corr} decreased from the original value of -632 to -690 mV, within 5 min, after which it remained constant, until after 2 h IT. After 3 h IT, with the initial value of -653 mV, E_{corr} increased to -620 mV. The authors have attributed the increase in E_{corr} to the positive direction of the protective corrosion film developed by FeS on the steel surface, which hindered Fe dissolution in the anodic region and/or reduced HER in the cathodic region. They have concluded that the formation of a FeS protective film was only possible with a longer IT (>/= 2 h), a pH range from 3 to 5, and a lower Ct of H_2S (</=0.04 mmol/dm^{-3}).

Inhibitive performances of corrosion scales on steel in a CO_2 environment

A study using EIS and surface characterization techniques has been conducted by [38], to investigate the influence of CO_2 corrosion scales on steel CR. Their results have shown that brine affected the rate and formation of protective corrosion scales on the steel surface, with a slower CR seen at 640 than at 64 mL. The study has found that corrosion scales formed under high or low pressure at different T were less protective than the ones under high pressure and T, resulting in more protective crystalline $FeCO_3$. In addition, at a certain pressure and T, low impedance was seen, for a CR of 1.51 mm/year, indicating either the absence of a protective layer or weak adhesion of the formed layer to the alloy surface (Figs. 10 and 11) [38].

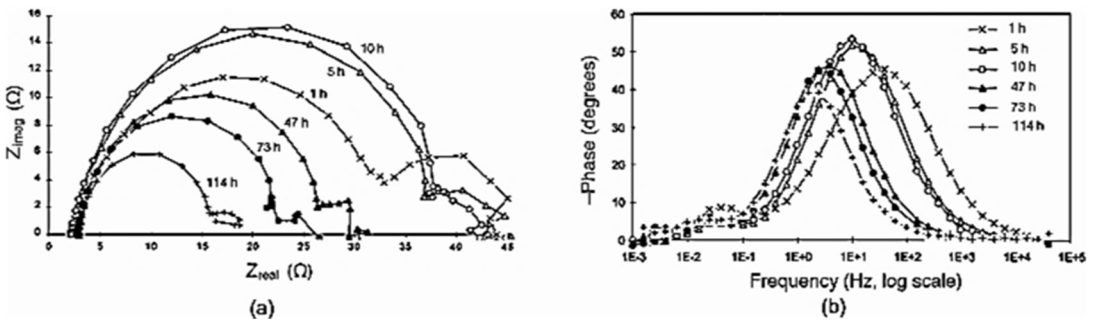

Figure 10: (a) Nyquist and **(b)** Bode phase graphs from an electrode exposed to 640 mL CO_2 saturated 3% NaCl for varying IT, at 1 ATM CO_2 and 30 °C.

A study on the influence of corrosion scales (Fe_3C) on the CR of MS, in aqueous CO_2 under turbulent flow conditions, has been conducted by [59]. The authors have found that, at pH 3.8, the $FeCO_3$ corrosion scale, caused by a thermodynamic reaction of Fe dissolution in H_2CO_3, was poorly formed, due to a short IT. With longer IT, CR increased, due to the larger area of Fe_3C residues and the partial protection offered by $FeCO_3$. At pH 5.5, CR increased with IT, due to unoxidized Fe_3C, which provided stronger electrochemical behavior than the poorly formed $FeCO_3$ corrosion scale. Furthermore, they have investigated the impact of HCO_3^- on Fe corrosion and passivation. Their findings have shown that the presence of HCO_3^- has significantly increased Fe dissolution in both pre-passive and active regions, leading to the formation of an iron complex. Pitting occurred during the

dissolution process, but CR was rapidly reduced by the formation of a protective and soluble Fe (III) complex: $Fe(CO_3)_2^{2-}$ [59].
In a study comparing ferrite-pearlite steel and dual-phase steel, it was found that A-R steel mainly contained Fe and Fe_3C, due to residual Fe_3C accumulation after anodic Fe dissolution. This led to increased anodic and cathodic Tafel slopes, indicating a shift in the electrochemical process (Figs. 11 (a-c)). Fe_3C accumulated on the steel surface triggered galvanic corrosion. Similar results were found for DP75 and DP80 steels, with higher i_{corr}, as IT increased from 0 to 72 h [104].

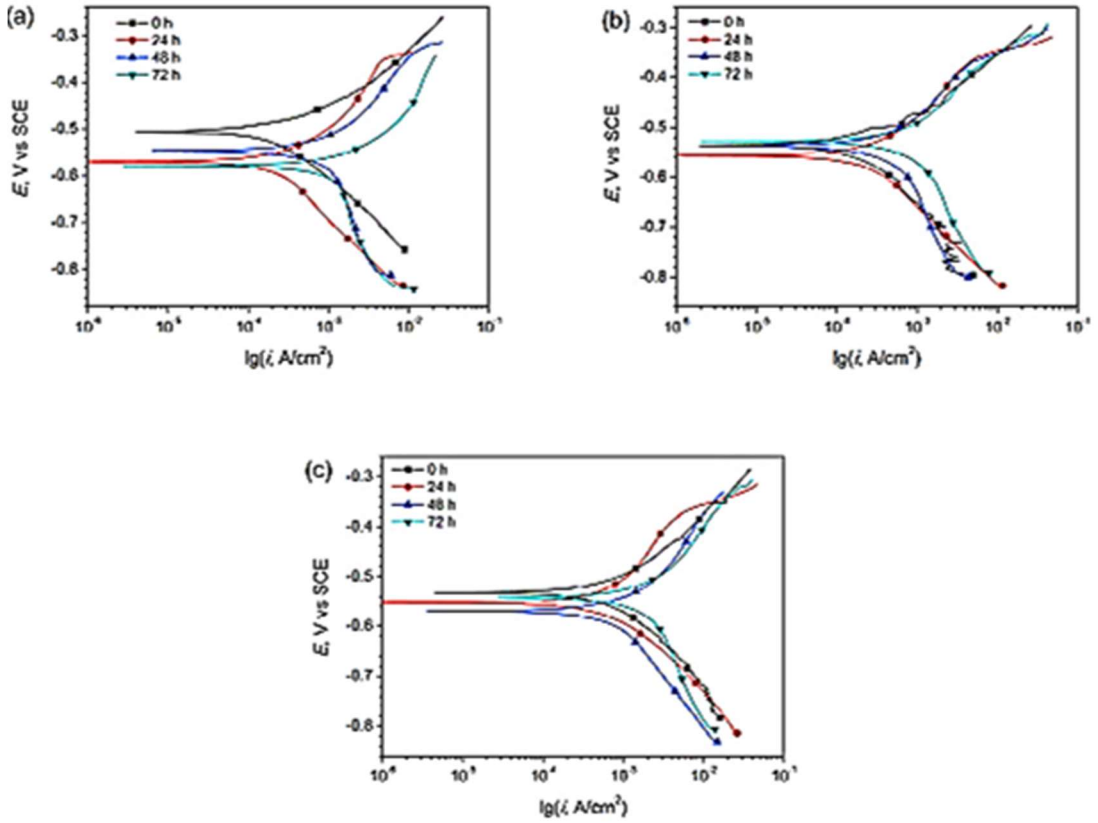

Figure 11: PDP curve diagrams for **(a)** A-R, **(b)** DP75, and **(c)** DP80 steels immersed in 10 wt.% NaCl with pH 0.85, at T of 30 ± 2 ºC.

Table 1 summarizes studies on the effect of corrosion scales on steel corrosion behavior in CO_2/H_2S environments.

Table 1: Summary of some literature studies on the influence of corrosion scales on steel corrosion behavior in CO_2/H_2S environments.

Material	Environment	Test conditions	Methods	Corrosion scales	Influence of corrosion scales on steel CR	Ref
X65 steel	Low supercritical CO_2 partial pressure	80 ºC	X-RD /SEM/EDS	$FeCO_3$	With longer IT, $FeCO_3$ corrosion scales reduced CR from 17 to 1.64 and 28 to 7.26 mm/yr, under low and supercritical CO_2 conditions.	[2]

X52 steel	3 wt.% NaCl saturated with high-pressure CO_2/ formation water	60 ºC/24 h/pH 6	LPR/WL/SEM/EDX/ X-RD	$FeCO_3$/ Fe_3C	$FeCO_3$ corrosion scales decreased CR from 29 to 21, 23 to 16.5, and 13 to 9.5 mm/yr, at CO_2 partial pressure of 60, 40, and 10 bars.	[7]
API 5L X65 /13Cr steel	Supercritical CO_2-water environment	0-120 h/50-80 ºC/03-80 barr	EDS/SEM/ X-RD/WL	y- $FeSO_3$. $3H_2O$/$FeCO_3$/ Fe_3C/ FeOOH/ $FeSO_4$	$FeCO_3$ corrosion scales, after 24 h, reduced CR from 1.0 to ~0.3 mm/yr.	[33]
CS	High pressure H_2S/CO_2 environment	40-60 ºC/ 0-1500 rpm/ 10000-50000 mg/L Cl^-	CFD/EDS/ SEM/WL	Fe_3C/ $FeCO_3$/FeS	FeS and $FeCO_3$ corrosion scales prevented the diffusion of corrosive species or solutions to the CS surface, decreasing CR.	[50]
CS	3wt.% NaCl saturated CO_2	pH 3.8 and 5.5/ 25 ºC/10-17 days/1000	EIS/PDP/ OCP	$FeCO_3$/ Fe_3C	The galvanic impact of Fe_3C residue increased CR from 3 to 4 mm/yr. $FeCO_3$ decreased CR.	[59]
X65 CS	3% NaCl saturated with CO_2	80 ºC/6-96 h	EIS/ OCP/ PDP/ X-RD/SEM/ profilometry/ NMR	Fe_3C/ partial and full $FeCO_3$	Fe_3C reduced CR from 4.84 to 3.25 mm/yr.	[65]
UNSK03014 CS/ UNSG413-1Cr and 3Cr	1% NaCl saturated CO_2 with H_2S	25-8ºC/20 h	WL/EIS/ OCP/LPR/ pH	$FeCO_3$ /FeS	$FeCO_3$ and Fe_3C reduced CR from 90 to 0.1 mm/yr.	[68]
X65 CS	$Cl^-/Ca^{2+}/(Mg^{2+}/CO_2$ saturated with NaCl	60 ºC/100 bar CO_2/6-9 h	SEM/FIB/ X-RD/EDX	$Fe_3C/FeCO_3$/ $Fe_xCa_yCO_3$/ $Fe_xMg_yCO_3$	Corrosion scales lowered CR to 80% after 96 h IT.	[70]
X65/1Cr/ 3Cr steel	1 wt.% NaCl saturated with CO_2	12 MPa CO_2/15h/ 120 bar/80 ºC	SEM/EDS/ EIS/OCP/ PDP	$FeCO_3$/FeS	Corrosion scales reduced CR from 90 to 4 mm/yr.	[90]
Q235 steel	CO_2/H_2S saturated with NaCl solution	80 $ml.min^{-1}$ (CO_2 and H_2S)/0 -7 days/3.5wt. % NaCl/60 ± 1 º C	EIS/ X-RD/ EDS/SEM/ XPS/OCP/ PDP/EIS/	FeS/$FeCO_3$	FeS and $FeCO_3$ corrosion scales reduced icorr value from 90.1 µA cm^2 and Ecorr from 0 TO 715 V after 7 days.	[95]
API 5L/ X65 CS	3.5wt.% NaCl saturated with CO_2/H_2S	50 and 150 ppm inhibitors for CO_2 and H_2S	EIS/OCP/ PDP/OES-	$FeCO_3$ (siderite)/ reduced FeS	FeS and $FeCO_3$ scales, with a 200 µm layer, reduced i and prevented corrosion from occurring.	[96]
N80 CS	Supercritical CO_2 oilfield produced water	1 M KCl/3L autoclave/ 60 ºC/ 0-36 h	EIS/ PDP, OCP/SEM/ EDS/GIX-RD/ GFN-*x*TB method	intermediate $Fe(OH_{ads})$/ Fe_3C/ $FeCO_3$	Fe_3C corrosion scale increased CR after 24 h. $FeCO_3$ scale, after 48 h, increased R_p and E_{corr}.	[98]
N80 CS	1% NaCl solution saturated with CO_2	1700 mL CO_2/35 ºC/ 2000	EDS/X-RD/ SEM/EIS/ WL	$FeCO_3$	$FeCO_3$ reduced CR from 15 to 1.5 mm/yr and increased R_p from 2.0 to	[99]
AISI 1020 CS	Supercritical CO_2 conditions with $NaHCO_3$ and NaCl	CO_2 (8 MPa)/0-/72h/25-60 ºC	EIS/OCP/ PDP/SEM/ EDS/ X-RD/ICP-AES	$Fe_3C/FeCO_3$	$FeCO_3$ scales mitigated localized corrosion by impeding the diffusion of reactant species.	[115]
CS	3% NaCl + diesel solution saturated with CO_2	50 ºC/12 h	LPR/EIS	$FeCO_3$	$FeCO_3$ scales contributed to an increase in R_p from 100 to 50000 ohm/cm^2	[165]

1018 CS	CO_2 saturated with 3 wt.% NaCl + 10 % diesels	50 ºC/24 h	SEM/AES/ EIS/PDP/ OCP	$FeCO_3$/FeOOH	$FeCO_3$ caused a slight decrease in R_{ct} value with increased time.	[166]
AISI 1018	CO_2/H_2S saturation	Synthetic NaCl/ 60 °C/	EIS/OCP/P DP	FeS	FeS reduced CR from 1.0 to 0.1 mm/yr.	[167]
X 65 pipeline steel	Supercritical CO_2 condition	50-130 º C/0.5-168 h	SEM/ X-RD/ EDS/EIS	$FeCO_3$	$FeCO_3$ decreased CR from 30 to 8.0) mm/yr after 170 h	[168]
P110/ N80/J55 steel	Produced water saturated with supercritical CO_2 condition	60-150 ºC pH 4-6	EDX/XPS/ SEM/ X-RD/WL	$FeCO_3/CaCO_3/\alpha$ -FeOOH	$FeCO_3$ decreased CR from 3.5 to 1.0, 2.5 to 1.0, and 2.2 to 0.8 mm/yr, at increased T and also time.	[169]

Research gaps and future perspectives

Literature research showed that steel corrosion in CO_2/H_2S environments has been extensively studied under simulated oilfield conditions over a short period. However, these studies do not accurately represent real-world scenarios in which these steels are exposed to various corrosive environments for extended periods. Crucial factors such as pressure, T, Ct, fluid dynamics, and chemical composition, which significantly influence the corrosion process, are often inadequately taken into account. Consequently, the duration and level of protection these films provide in practical applications may differ from what is seen in controlled experiments. Therefore, conducting research under realistic conditions is essential to gain a deeper understanding of the effects of corrosion products on steel in CO_2/H_2S environments.

The presence of deposits on CS and low alloy steels in a CO_2/H_2S environment can reduce the effectiveness of corrosion inhibitors used in the oil and gas industry. The interaction between these scales and inhibitors can either enhance or hinder their adsorption and performance capabilities. This interaction depends on the type and nature of the corrosion product and its affinity to the underlying substrate. Porous corrosion products can allow for the penetration of corrosive agents and trigger local corrosion. Therefore, it is crucial to thoroughly study the effects of corrosion product scales, their inhibitory behavior, and their interaction with corrosion inhibitors. It is important to conduct molecular studies on interactions between corrosion scales and alloy surfaces. Computational simulation techniques can deepen our understanding of the formation, absorption, and inhibition effects of corrosion deposits. In addition, the composition, type, and form of corrosion products can significantly influence their protective properties. Research into phase transitions could lead to optimized corrosion prevention measures in practical applications.

To gain a deeper understanding of the process of corrosion formation and removal, a comprehensive assessment is required to evaluate the influence of flow rate on the formation of corrosion products. This evaluation should also take into account the type of protection that the corrosion products can provide to the underlying alloy. Given the rapid kinetics associated with the formation of mackinawite corrosion scale on CS and low alloy steel surfaces, particularly in H_2S

environments, further studies are required to investigate its growth, properties, response to corrosion inhibitors under various conditions, and understand subsequent removal with chemicals and/or mechanical methods.

The presence of corrosion scales on alloy surfaces significantly affects CS and low alloy steel corrosion behavior. Formation of corrosion scales on steel surfaces can also lead to adverse effects such as reduced corrosion resistance, increased flow resistance, compromised mechanical properties, higher maintenance and operating costs, and reduced heat transfer efficiency. To ensure the longevity and performance of CS components in various industrial applications, it is important to control and minimize scale formation. To achieve this, effective tactics include modifying metals, implementing protective barriers, adhering to environmental guidelines, adjusting engineering designs, using corrosion inhibitors and sacrificial coatings, treating chemicals, managing water resources, and conducting more thorough facility and equipment monitoring and inspections [170].

Conclusion

CS and low alloy steel corrosion pose serious problems to the oil and gas sector, potentially affecting the structures, properties, and operational efficiency of these materials. This can lead to equipment and system failures, safety issues, damage, and environmental pollution. CO_2/H_2S corrosion produces various types of scales on steel surfaces through anodic dissolution of ferrite, cathodic HER, or oxidant reduction. The formation and nature of scales formed on steel surfaces in a CO_2/H_2S environment depend on some factors such as pH, Ct, and dominant gas. This review took a holistic approach to examining the formation and inhibitory effect of corrosion product scales on steel surfaces in CO_2/H_2S environments. Particular emphasis was put on Fe_3C, $FeCO_3$, and FeS, as the most commonly reported scale deposits, since they can reduce CR and increase the E_{corr} of steel.

Acknowledgment

The authors gratefully acknowledge the financial support from the World Bank-funded second Higher Education Centers of Excellence for Development Impact (ACE-Impact) Project – P16906-4A No 6510-NG and Federal University of Technology, Owerri, Imo State, Nigeria.

Declaration of competing interest

The authors declare that there is no conflict of interest.

Authors' contributions

C. I. Ekeocha: conceptualization, methodology, reviewing, and writing - original draft. **I. B. Onyeachu:** data curation, editing, and supervision, **I. I. Etim:** visualization, writing – reviewing, editing, and supervision; **I. N. Uzochukwu:** writing - original draft and reviewing. **E. E. Oguzie**: conceptualization, supervision, editing, resources, and project administration.

Abbreviations
ATM: atmospheres (meters of resistance)
CFD: Computational Fluid Dynamics
CH_3COOH: acetic acid
CO_2: carbon dioxide
CO_3^{2-}: carbonate
CR: corrosion rate
CS: carbon steel
Ct: concentration
E_{corr}: corrosion potential
EDS: Electron dispersed spectroscopy
EIS: electrochemical impedance spectroscopy
Fe_3C: iron carbide
Fe_3O_4: magnetite
Fe_9S_8: kansite
$FeCO_3$: iron (II) carbonate (siderite)
$Fe(HCO_3)_2$: iron (II) hydrogen carbonate
$FeHS^+_{(aq)}$: iron (II) hydrosulfide ion
FeS: iron sulfide (mackinawite)
$FeSO_3 \cdot 2H_2O$: iron(II) sulfate
$Fe_xCa_yCO_3$: iron-calcium carbonate
$Fe_xMg_yCO_3$: iron-magnesium carbonate
GFN-*x*TB: Geometry Frequency Non-covalent extended Tight Binding
GIX-RD: Grazing Incidence X-ray Diffraction
H_2CO_3: carbonic acid
H_2S: hydrogen sulfide
H_2SO_4: sulfuric acid
HCO_3^-: bicarbonate
HER: hydrogen evolution reaction
HS^-: bisulphide
i: current density
i_{corr}: corrosion current density
ICP-AES: Inductively Coupled Plasma-Atomic Emission Spectroscopy
IOB: iron-oxidizing bacteria
IT: immersion time
KCl: potassium chloride
LPR: Linear Polarization Resistance
MPa: megapascals
MS: mild steel
NaCl: sodium chloride
$NaHCO_3$: sodium bicarbonate
NMR: nuclear magnetic resonance
OCP: open circuit potential
OES: Optical Emission Spectrometry
PDP: Potentiodynamic Polarization
ppm: part per million

R_{ct}: charge transfer resistance
RDS: rate-determining step
R_p: polarization resistance
Rpm: rotation per minute
SEM: scanning electron microscopy
T: temperature
WL: weight loss
X-RD: x-ray diffraction

Symbols definition
µm: micrometer

References

1. Bharatiya U, Gal P, Agrawal A et al. Effect of Corrosion on Crude Oil and Natural Gas Pipeline with Emphasis on Prevention by Eco-friendly Corrosion Inhibitors. A Comprehensive Review. J Bio- Tribo- Corros. 2019;(5)2:1-12. https://doi.org/10.1007/s40735-019-0225-9
2. Zhang Y, Pang X, Qu S et al. Discussion of the CO_2 corrosion mechanism between low partial pressure and supercritical condition. Corros Sci. 2012;(59):186-197. https://doi.org/10.1016/j.corsci.2012.03.006.
3. Kermani MB, Morshed A. Carbon dioxide corrosion in oil and gas production - A compendium. Corrosion. 2003;(59)8:659-683. https://doi.org/10.5006/1.3277596
4. Burkle DP. Understanding the formation of protective $FeCO_3$ on carbon steel pipelines during CO_2. Corrosion. 2017;(4):1-335. PhD thesis, University of Leeds https://core.ac.uk/works/8600770/
5. Jafar MA. Global Impact of Corrosion: Occurrence, Cost and Mitigation. Glob J Eng Sci. 2020;(5)4:0-4. https://doi.org/10.33552/gjes.2020.05.000618
6. Paolinelli LD, Pérez T, Simison SN. The effect of pre-corrosion and steel microstructure on inhibitor performance in CO_2 corrosion. Corros Sci. 2008;(50)9:2456-2464. https://doi.org/10.1016/j.corsci.2008.06.031
7. Mustafa AH, Ari-Wahjoedi B, Ismail MC. Inhibition of CO_2 Corrosion of X52 Steel by Imidazoline-Based Inhibitor in High-Pressure CO_2-Water Environment. J Mat Engr Perf. 2012;22(6):1748-1755. https://doi.org/10.1007/s11665-012-0443-5
8. Hu J, Xiong Q, Chen L et al. Corrosion inhibitor in CO_2-O_2-containing environment: Inhibition effect and mechanisms of Bis(2-ethyl hexyl) phosphate for the corrosion of carbon steel. Corros Sci. 2020;179:109173. https://doi.org/10.1016/j.corsci.2020.109173
9. Xhanari K, Wang Y, Yang Z et al. A Review of Recent Advances in the Inhibition of Sweet Corrosion. Chem Rec. 2021;(7):1845-187. https://doi.org/10.1002/tcr.202100072

10. Unueroh U, Omonria G, Efosa O et al. Pipeline Corrosion Control in Oil and Gas Industry: a Case Study of NNPC/PPMC System 2a Pipeline. Niger J Tech. 2016;(35)2:317. https://doi.org/10.4314/njt.v35i2.11
11. El Ibrahimi B, Jmiai A, Bazzi L et al. Amino acids and their derivatives as corrosion inhibitors for metals and alloys. Arab J Chem. 2020;(13)1:740-771. https://doi.org/10.1016/j.arabjc.2017.07.013
12. Sastri VS. Challenges in Corrosion, Costs, Causes, Consequences and Control. General and Introductory Material Science Corrosion. 2015. ISBN: 978-1-118-52210-3. https://doi.org/10.1002/9781119069638.ch2
13. Prabha SS, Rathish RJ, Dorothy R. Corrosion Problems in Petroleum Industry and their Solution. Eur Chem Bull 2014;(3)3:300-307. https://doi.org/10.17628/ECB.2014.3.300-307
14. Cheng XL, Ma HY, Zhang JP et al. Corrosion of Iron in Acid Solutions with Hydrogen Sulfide. Corrosion. 1998;(54)5:369-375. https://doi.org/10.5006/1.3284864
15. Wolthers M, Van Der Gaast SJ, Rickard D. The structure of disordered mackinawite. Amer Mineral. 2007;(88):11-12. https://doi.org/10.2138/am-2003-11-124
16. Tribollet B, Kittel J, Meroufel A et al. Corrosion mechanisms in aqueous solutions containing dissolved H_2S. Part 2: Model of the cathodic reactions on a 316L stainless steel rotating disc electrode. Electrochim Acta. 2014;(124)1:46-51. https://doi.org/10.1016/j.electacta.2013.08.133
17. Ding Y, Brown B, Young D et al. Effectiveness of an imidazoline-type inhibitor against CO_2 corrosion of mild steel at higher temperatures. Corros Conf Expo. 2018;(11622):1-22.
18. Kermani M.B, Harrop D. The impact of corrosion on the oil and gas industry. SPE Prod Facil. 1996;(11)3:186-190. https://doi.org/10.2118/29784-PA
19. Nordsveen M, Nešić S, Nyborg R et al. A mechanistic model for carbon dioxide corrosion of mild steel in the presence of protective iron carbonate films - Part 1: Theory and verification. Corrosion. 2003;(59)5:443-456. https://doi.org/10.5006/1.3277576
20. Ohfuji H, Rickard D. High-resolution transmission electron microscopic study of synthetic nanocrystalline mackinawite. Earth Planet Sci Lett. 2006;(241)1-2: 227-233. https://doi.org/10.1016/j.epsl.2005.10.006
21. Skinner BJ, Erdr RC, Grimaldi FS. Greigite, the thio-spinel of iron; is a new mineral. Amer Mineral. 1964(49):543-55. URL: http://www.minsocam.org/MSA/AmMin/TOC/
22. Rickard DA. New Sedimentary Pyrite Formation Model. Mineral Mag. 1994;(58A):2772-773. https://doi.org/10.1180/minmag.1994.58a.2.138
23. Spender MR, Coey MD, Morrish AH. The Magnetic Properties and Mössbauer Spectra of Synthetic Samples of Fe_3S_4. Canad J Phys. 1972;50(19):2313-2326. https://doi.org/10.1139/P72-306
24. Kahyarian A, Nesic S. H_2S corrosion of mild steel: A quantitative analysis of the mechanism of the cathodic reaction. Electrochim Acta. 2019;(297):676-684. https://doi.org/10.1016/j.electacta.2018.12.029

25. Ma H, Cheng X, Chen S et al. An ac impedance study of the anodic dissolution of iron in sulfuric acid solutions containing hydrogen sulfide. J Electroanalyt Chem 1998;(451):11-17 http://dx.doi.org/10.1016/S0022-0728(98)00081-3
26. Khoma MS, Ivashkiv VR, Chuchman MR et al. Corrosion cracking of environmental differences in the structural structure hydrogen sulfide environment under static load corrosion cracking of carbon steels of different structures in the modeling of a high-pressure turbine blade. Proceed Struct Integr. 2018;(13):2184-2189. https://doi.org/10.1016/j.prostr.2018.12.143
27. Wang LM, Lu M. The Effect of Temperature on the Hydrogen Permeation of Pipeline Steel in Wet Hydrogen Sulfide Environments. 2018;(13):915-924. https://doi.org/10.20964/2018.01.52
28. Zhao W, Zou Y, Matsuda K et al. Characterization of the effect of hydrogen sulfide on the corrosion of X80 pipeline steel in saline solution. Eval Program Plann. 2015;(102):455-468. https://doi.org/ 10.1016/j.corsci.2015.10.038
29. Meyer FH, Riggs OL, McGlasson RL et al. Corrosion products on steel in H_2S. Thirteen Annual Conf Nat Ass Corro Eng. 1957;(3):11-15.
30. Gu T, Su P, Liu X et al. A Composite Inhibitor Used in Oilfield. MA-AMPS and Imidazoline. J Pet Sci Engr. 2013;102:41-46. https://doi.org/10.1016/j.petrol.2013.01.014
31. Jiashen Z, Jingmao Z. Control of Corrosion by Inhibitors in Drilling Muds Containing High Concentration of H_2S. Corrosion. 1993;(49)2:170-174. ISSN 0010-9312. https://doi.org/10.5006/1.3299211
32. Wei L, Zhang Y, Pang X et al. Corrosion behaviors of steels under supercritical CO_2 conditions. Corros Rev. 2014;(33)3-4:151-174. https://doi.org/10.1515/corrrev-2014-0067
33. Choi YS, Nesic S, Young D. Effect of impurities on the corrosion behavior of CO_2 transmission pipeline steel in supercritical CO_2-water environments. Environ Sci Technol. 2010;(44)23:9233-9238. https://doi.org/10.1021/es102578c
34. Gao K, Yu F, Pang X et al. Mechanical properties of CO_2 corrosion product scales and their relationship to corrosion rate. Corros Sci. 2008;(50)10:2796-2803. https://doi.org/10.1016/j.corsci.2008.07.016
35. López DA, Pérez T, Simison SN. The influence of microstructure and chemical composition of carbon and low alloy steels in CO_2 corrosion. A state-of-the-art appraisal. Mater Des. 2003;(24)8:561-575. https://doi.org/10.1016/S0261-3069(03)00158-4
36. Moiseeva LS. Carbon dioxide corrosion of oil and gas field equipment. Protect Met. 2005;(41)1:76-83. https://doi.org/10.1007/s11124-005-0011-6
37. Ogundele GI, White WE. Some Observations on Corrosion of Carbon Steel in Aqueous Environments Containing Carbon Dioxide. Corrosion. 1986;(42)2:71-78. https://doi.org/10.5006/1.3584888

38. Kinsella B, Tan YJ, Bailey S. Electrochemical Impedance Spectroscopy and Surface Characterization Techniques to Study Carbon Dioxide Corrosion Product Scales. Corrosion. 1998;(54)10:835-842. https://doi.org/10.5006/1.3284803
39. López DA,Simison SN, De Sánchez SR. The influence of steel microstructure on CO_2 corrosion. EIS studies on the inhibition efficiency of benzimidazol. Electrochim Acta. 2003;(48)7:845-854. https://doi.org/10.1016/S0013-4686(02)00776-4
40. Heuer JK, Stubbins JF. An XPS characterization of $FeCO_3$ films from CO_2 Corrosion. Corros Sci. 1999;(41)7:1231-1243. https://doi.org/10.1016/S0010-938X(98)00180-2
41. Villarreal J, Laverde D, Fuentes C. Carbon-steel corrosion in multiphase slug flow and CO_2. Corros Sci. 2006;(48)9:2363-2379. https://doi.org/10.1016/j.corsci.2005.09.003
42. Rogers WF, Rowe Jr A. Corrosion Effects of Hydrogen Sulphide and Carbon Dioxide in Oil Production. World Petrol Congr. 1955;(3).
43. Sun W, Nes S. Kinetics of Corrosion Layer Formation. Part 2 — Iron Sulfide and Mixed Iron Sulfide/Carbonate Layers in Carbon Dioxide/Hydrogen Sulfide Corrosion. Corrosion. 2008;64(7):586-599. https://doi.org/10.5006/1.3278494
44. Wang P, Wang J, Zheng S et al. Effect of H_2S/CO_2 partial pressure ratio on the tensile properties of X80 pipeline steel. Int J Hydrogen Energy. 2015;40(35):11925-11930. https://doi.org/10.1016/j.ijhydene.2015.04.114
45. Brown BN, Nesic S. C2012-0001559. NACE Internat. 2012;(3):1-22 https://www.icmt.ohio.edu/documents/NACE2012/C2012-0001559.pdf
46. Sardisco JB, Pitts RE. Corrosion of Iron in an H_2S-CO_2-H_2O System Composition and Protectiveness of the Sulfide Film as a Function of pH 1965; 21(110):350-354. https://doi.org/10.5006/0010-9312-21.11.350
47. Revie W, Uhlig HH. Corrosion and Corrosion Control: An Introduction to Corrosion Science and Engineering. John Wiley and Sons Inc. Print 2008:1-490. https://doi.org/10.1002/97804702777270
48. Sun W, Nesic S. Kinetics of Corrosion Layer Formation Corrosion. Part 1-Iron Carbonate Layer in Carbon Dioxide Corrosion. Corrosion. 2008;(64)4:334-346. https://doi.org/10.5006/1.3278477
49. Plennevaux C, Kittel J, Fregonese M et al. Contribution of CO_2 on hydrogen evolution and hydrogen permeation in low alloy steels exposed to H_2S environment. Electrochem Commun. 2013;(26)1:17-20. https://doi.org/10.1016/j.elecom.2012.10.010
50. Zhang GA, Zeng Y, Guo YP et al. Electrochemical corrosion behavior of carbon steel under dynamic high-pressure H_2S/CO_2 environment. Corros Sci. 2012;(65):37-47. https://doi.org/10.1016/j.corsci.2012.08.007
51. Rickard D. Kinetics of pyrite formation by the H_2S oxidation of iron (II) monosulfide in aqueous solutions between 25 and 125°C: The rate Eq. Geochim Cosmochim Acta. 1997;61(1):115-134. https://doi.org/10.1016/s0016-7037(96)00321-3

52. Schmitt GA, Mueller M, Papenfuss M, et al. Understanding Localized CO_2 Corrosion of Carbon Steel from Physical Properties of Iron Carbonate Scales. Corrosion. 1999;(4)25.
53. Smith SN, Pacheco JL. Prediction of corrosion in slightly sour environments. Int Corr Conf . Expo. 2002;(4):3. Paper 02241.
54. Smith SN. Current Understanding of Corrosion Mechanisms Due to H_2S in Oil and Gas Production Environments. NACE Int Corros Conf Expo. 2015. Paper No. 5485.
55. Smith SN. Joosten M Corrosion of Carbon Steel by H_2S in CO_2 Containing Oilfield Environments. NACE- Int Corros Conf . Expo 2006. Paper No. 06115.
56. De Motte R, Basilico E, Mingant R, et al. A study by electrochemical impedance spectroscopy and surface analysis of corrosion product layers formed during CO_2 corrosion of low alloy steel. Corros Sci. 2020;(172)4:108666. https://doi.org/10.1016/j.corsci.2020.108666
57. Motte D. In situ SR-X-RD study of $FeCO_3$ precipitation kinetics onto carbon steel in CO_2-containing environments: The influence of brine pH. Electrochem Acta. 2017(255):127-144. https://doi.org/10.1016/j.electacta.2017.09.138
58. Farelas F, Brown B, Nesic S. Iron carbide and its influence on the formation of protective iron carbonate in CO_2 corrosion of mild steel. NACE - Inter Corros Conf Expo Ser. 2013. Paper No. 229.
59. Mora-Mendoza JL, Turgoose S. Fe_3C influence on the corrosion rate of mild steel in aqueous CO_2 systems under turbulent flow conditions. Corros Sci. 2002;(44)6:1223-1246. https://doi.org/10.1016/S0010-938X(01)00141-X
60. Davies DH, Burstein GT. The Effects of Bicarbonate on the Corrosion and Passivation of Iron. Corrosion. 1980;36(8)416-422. https://doi.org/10.5006/0010-9312-36.8.416
61. Ma H, Cheng X, Li G et al. The influence of hydrogen sulfide on iron corrosion under different conditions. Corros Sci. 2000;(42):1669-1683. https://doi.org/10.1016/S0010-938X(00)00003-2
62. Sun W. Kinetics of Iron carbonate and iron sulfide scale formation in CO_2/H_2S corrosion. A PhD dissertation. 2006.
63. Bai P, Zheng S, Zhao H et al. Investigations of the diverse corrosion products on steel in a hydrogen sulfide environment. Corros Sci. 2014;(87):397-406. https://doi.org/10.1016/j.corsci.2014.06.048
64. Liu X, Okafor PC, Zheng YG. The inhibition of CO_2 corrosion of N80 mild steel in single liquid phase and liquid/particle two-phase flow by aminoethyl imidazoline derivatives. Corros Sci. 2009;(51)4:744-751. https://doi.org/10.1016/j.corsci.2008.12.024
65. Shamsa A, Barker R. Hua Y, et al. Impact of corrosion products on the performance of imidazoline corrosion inhibitor on X65 carbon steel in CO_2 environments. Corros Sci. 2021;(185)109423. https://doi.org/10.1016/j.corsci.2021.109423

66. Zhang C, Asl VZ, Lu Y et al. Investigation of the corrosion inhibition performances of various inhibitors for carbon steel in CO_2 and CO_2/H_2S environments. Corr Eng Sci Technol. 2020;5(7):1-8. https://doi.org/10.1080/1478422X.2020.1753929
67. Lu Y, Wang W, Zhang C. A Novel Imidazoline Derivative Used as an Effective Corrosion Inhibitor for Carbon Steel in a CO_2/H_2S Environment. Int J Electrochem Sci. 2019;(14):8579-8594. https://doi.org/10.20964/2019.09.06
68. Nor AM, Suhor MF. Strategies for Corrosion Inhibition of Carbon Steel Pipelines Under Supercritical CO_2/H_2S Environments. Corrosion. 2019;(75)10:1156-1172. https://doi.org/10.5006/2765
69. Verma C, Olasunkanmi LO, Ebenso EE et al. Substituents effect on corrosion inhibition performances of organic compounds in aggressive ionic solution: A review. J Mol Liq. 2017;251:1-78. https://doi.org/10.1016/j.molliq.2017.12.055
70. Hua Y, Shamsa A, Barker R, et al. Protectiveness, morphology, and composition of corrosion products formed on carbon steel in Cl^-, $Ca^{2+,}$ and Mg^{2+} presence in high-pressure CO_2 environments. Appl Surf Sci. 2018;455;667-682. https://doi.org/10.1016/j.apsusc.2018.05.140
71. Perez TE. Corrosion in the oil and gas industry: An increasing challenge for materials. JOM. 2013;(65)8:1033-1042. https://doi.org/10.1007/s11837-013-0675-3
72. Wei L, Zhang Y, Pang X. Corrosion behaviors of steels under supercritical CO_2 conditions. Corros Rev. 2015;(33)3-4:151-174. https://doi.org/10.1515/corrrev-2014-0067
73. Crolet J, Bonis M. Prediction of the Risks of CO_2 Corrosion in the Oil and Gas Wells. SPE Prod Eng. 1991;(6):449-453. https://doi.org//10.2118/20835-PA
74. Li T, Yang Y, Gao K. Mechanism of protective film formation during CO_2 corrosion of X65 pipeline steel. J Uni Sci Technol Beijing. 2008;(15)6:702-706. https://doi.org/10.1016/S1005-8850(08)60274-1
75. Groysman A. Corrosion problems and solutions in oil, gas, refining and petrochemical industry. Koroz Ochr Mater. 2017;(61)3:100-117. https://doi.org/10.1515/kom-2017-0013
76. Rickard D, Griffith A, Oldroyd A et al. The composition of nanoparticulate mackinawite, tetragonal iron(II) monosulfide. Chem Geol. 2006;(235)3-4:286-298. https://doi.org/10.1016/j.chemgeo.2006.07.004
77. John RC, Pelton AD, Young AL et al. Assessing corrosion in oil refining and petrochemical processing. Mat Res. 2004;(7)1:163-173. https://doi.org/10.1590/s1516-14392004000100022
78. Foss M, Gulbrandsen E. Effect of Corrosion Inhibitors and Oil on Carbon Dioxide Corrosion and Wetting of Carbon Steel with Ferrous Carbonate Deposits. Corrosion. 2009;65(1):3-14. https://doi.org/10.5006/1.3319113

79. Tomson MB, Rice U, Johnson ML. How Ferrous Carbonate Kinetics Impacts Oilfield Corrosion. SPE Int Conf Oil Chem-21025-MS. 1991;(2):257-264. https://doi.org/10.2118/21025-MS
80. Yaro AS, Abdul-Khalik AR, Khadom AA. Effect of CO_2 corrosion behavior of mild steel in oilfield produced water. J Loss Prev Proc Ind. 2015;(38):24-38. https://doi.org/10.1016/j.jlp.2015.08.003
81. Pandarinathan V, Lepková K, Van Bronswijk W. Chukanovite ($Fe_2(OH)_2CO_3$) identified as a corrosion product at sand-deposited carbon steel in CO_2-saturated brine. Corros Sci. 2014;(85):26-32. https://doi.org/10.1016/j.corsci.2014.03.032
82. Foss M, Gulbrandsen E, Sjoblom J. Oil Wetting and Carbon Dioxide Corrosion Inhibition of Carbon Steel with Ferric Corrosion Products Deposits. Corrosion. 2010;(66)2:1-11. https://doi.org10.5006/1.3319662/
83. Wang C, Neville A. Inhibitor performance on corrosion and erosion/corrosion under turbulent flow with sand and CO_2 - An AC impedance study. SPE Prod Oper. 2008;(23)2:215-220. https://doi.org/10.2118/100441-pa
84. Schreiner WH, De Sá SR. The influence of inhibitors molecular structure and steel microstructure on corrosion layers in CO_2 corrosion: An XPS and SEM characterization. Appl Sur Sci. 2004;(236):77-97. https://doi.org/10.1016/j.apsusc.2004.03.247
85. Hua Y, Xu S, Wang Y et al. The formation of $FeCO_3$ and Fe_3O_4 on carbon steel and their protective capabilities against CO_2 corrosion at elevated temperature and pressure. Corros Sci. 2019;(157)6:392-405. https://doi.org/10.1016/j.corsci.2019.06.016
86. El-Lateef HMA, Abbasov MV, Aliyeva LI et al. Corrosion Protection of Steel Pipelines Against CO_2 Corrosion-A Review. Chem J. 2012;(2)2:52-63 ISSN 2049-954X www.scientific-journals.co.uk
87. Sun C, Sun J, Wang Y et al. Synergistic effect of O_2, H_2S, and SO_2 impurities on the corrosion behavior of X65 steel in water-saturated supercritical CO_2 system. Eval Program Plann. 2016;(107):193-203. https://doi.org/10.1016/j.corsci.2016.02.032
88. Jiang X, Zheng YG, Qu DR. Effect of calcium ions on pitting corrosion and inhibition performance in CO_2 corrosion of N80 steel. Corros Sci. 2006;(48):3091-3108. https://doi.org/10.1016/j.corsci.2005.12.002
89. Paolinelli LD, Pérez T, Simison SN. The incidence of chromium-rich corrosion products on the efficiency of an imidazoline-based inhibitor used for CO_2 corrosion prevention. Mater Chem Phys. 2011;(126)3:938-947. https://doi.org/10.1016/j.matchemphys.2010.12.001
90. Choi YS, Hassani S, Vu TN et al. Effects of H_2S on the corrosion behavior of pipeline steels under supercritical and liquid CO_2 environments. Corrosion. 2015;(72)8:999-1009. http://dx.doi.org/10.5006/2026
91. Neville A, Wang C. Erosion – corrosion mitigation by corrosion inhibitors-An assessment of mechanisms. Wear. 2009;(267):195-203. https://doi.org/10.1016/j.wear.2009.01.038

92. El-Lateef HM, Abbasov VM, Aliyeva LI et al. Corrosion Protection of Steel Pipelines Against CO_2 Corrosion-A Review. Chem J. 2012;(2)2:52-63. www.scientific-journals.co.uk
93. Shamsa A, Barker R, Hua Y et al. Performance evaluation of an imidazoline corrosion inhibitor in a CO_2-saturated environment with emphasis on localized corrosion. Corros Sci. 2020;(176)9:108916. https://doi.org/10.1016/j.corsci.2020.108916
94. Gulbrandsen E, Nesic S, Stangeland A et al. Effect of Precorrection Localized on the Performance of Inhibitors for CO_2 Corrosion of Carbon Steel. NACE-Int Corros Conf Ser. 1998;(13):98013. ISSN 0361-4409.
95. Zhang C, Zhao J. Effects of Pre-Corrosion on the Corrosion Inhibition Performance of Three Inhibitors on Q235 Steel in CO_2/H_2S Saturated Brine Solution. Int J Electrochem Sci. 2017;(12):9161-9179. https://doi.org/10.20964/2017.10.51
96. Javidi M, Chamanfar R, Bekhrad S. Investigation of the Efficiency of Corrosion Inhibitor in CO_2 Corrosion of Carbon Steel in the Presence of Iron Carbonate Scale. J Nat Gas Sci Eng. 2019;61:197-205. https://doi.org/10.1016/j.jngse.2018.11.017
97. Eliyan FF, Alfantazi A. On the theory of CO_2 corrosion reactions-Investigating their interrelation with the corrosion products and API-X100 steel microstructure. Corros Sci. 2014:1-14. https://doi.org/10.1016/j.corsci.2014.04.055
98. Hou BS, Zhang QH, Li Y et al. Influence of corrosion products on the inhibition effect of pyrimidine derivative for the corrosion of carbon steel under supercritical CO_2 conditions. Corros Sci. 2020;(166):108442. https://doi.org/10.1016/j.corsci.2020.108442
99. Liu D, Qiu YB, Tomoe Y et al. Interaction of inhibitors with corrosion scale formed on N80 steel in CO_2-saturated NaCl solution. Mat Corros. 2011(12):1153-1158. https://doi.org/ 10.1002/maco.201106075
100. Zhong D, Liguo Z, Yicong T. et al. Investigation on Corrosion of Insulation Tubing Steel in HTHP Steam and Flue Gas Co-Injected to Enhance Heavy Oil Production. SPE Asia Pacific Oil Gas Conf Expo. 2013. SPE-165820-MS. https://doi.org/10.2118/165820-MS
101. Lazzari L, Pedeferri M. Corrosion Science and Engineering. Eng Mat. 2018. ISBN 978-3-319-97624-2. https://doi.org/ 10.1007/978-3-319-97625-9
102. Basilico E, Fregonese M, Marcelin S. The effect of chemical species on the electrochemical reactions and corrosion product layer of carbon steel in CO_2 aqueous environment: A review. Mat Corr. 2021;(1):1-16. https://doi.org/10.1002/maco.202012118
103. Xiang, Y, Long Z L, Li C et al. Inhibition of N80 steel corrosion in impure supercritical CO_2 and CO_2-saturated aqueous phases by using imino inhibitors. Int J Green Gas Cont. 2017;(63)4:141-149. https://doi.org/10.1016/j.ijggc.2017.05.010

104. Hao X, Zhao X, Chen X et al. Comparative study on corrosion behaviors of ferrite-pearlite steel with dual-phase steel in the simulated bottom plate environment of cargo oil tanks. J Mat Res Technol. 2021;(12):399-411. https://doi.org/10.1016/j.jmrt.2021.02.095
105. Zhang GA, Cheng YF. Localized corrosion of carbon steel in a CO2-saturated oilfield formation water. Electrochem Acta. 2011;(56)3:1676-1685. https://doi.org/10.1016/j.electacta.2010.10.059
106. De Waard C, Milliams DE. Carbonic Acid Corrosion of Steel. Corrosion. 1975;(31)5:177-181. https://doi.org/10.5006/0010-9312-31.5.177
107. Sardisco JB, Pitts RE. Corrosion of Iron in an H_2S-CO_2-H_2O System Composition and Protectiveness of the Sulfide Film as a Function of pH. Corrosion. 1965;(21)11:350-354. https://doi.org/10.5006/0010-9312-21.11.350
108. Koteeswaran M. CO_2 and H_2S Corrosion in Oil Pipelines. Master thesis University of Stavanger. 2010;(6):1-79.
109. Zhang N, Zeng D, Zhang Z et al. Effect of flow velocity on pipeline steel corrosion behavior in H_2S/CO_2 environment with sulfur deposition. Corros Eng Sci Technol. 2018;(0):1-8. https://doi.org/10.1080/1478422X.2018.1476818
110. Lucio-Garcia MA, Gonzalez-Rodriguez JG, Casales M et al. Effect of heat treatment on H_2S corrosion of a micro-alloyed C-Mn steel. Corros Sci. 2009;(51)10:2380-2386. https://doi.org/10.1016/j.corsci.2009.06.022
111. Cervantes AT, Cruz MD, Aguilar MAD et al. Effect of Flow Rate on the Corrosion Products Formed on Traditional and New Generation API 5L X-70 in a Sour Brine Environment. Int J Electrochem Sci. 2015;(10)4:2904-2920. https://doi.org/10.1016/S1452-3981(23006506-9
112. Wang X, Xu J, Sun C et al. Effect of oilfield-produced water on corrosion of the pipeline. Int J Electrochem Sci. 2015;(10)10:8656-8667. https://doi.org/10.1016/S1452-3981(23)11125-4
113. Li W, Jing J, Sun J et al. Investigation of the Corrosion Characteristics and Corrosion Inhibitor Action on J55 Steel in Produced Water. Sustainability (Switzerland). 2023;(15)4:3355. https://doi.org/10.3390/su15043355
114. Song Y, Jiang G, Chen Y et al. Effects of chloride ions on corrosion of ductile iron and carbon steel in soil environments. Sci Rep. 2017;(6):1-13. https://doi.org/10.1038/s41598-017-07245-1
115. Zhang S, Hou L, Du H et al. A study on the interaction between chloride ions and CO_2 towards carbon steel corrosion. Corros Sci. 2020;(2):108531. https://doi.org/10.1016/j.corsci.2020.108531
116. Bockris JOM, Drazic D, Despic AR. The electrode kinetics of the deposition and dissolution of iron. Electrochim Acta. 1961;(4)2-4:325-361. https://doi.org/10.1016/0013-4686(61)80026-1
117. Ogundele GI, White WE. Observations on the Influences of Dissolved Hydrocarbon Gases and Variable Water Chemistries on Corrosion of an Api-L80 Steel. Corrosion. 1987;(43)11:665-673. https://doi.org/10.5006/1.3583847

118. Han J, Zhang J, Carey JW. Effect of bicarbonate on corrosion of carbon steel in CO_2 saturated brines. Int J Green Gas Cont. 2011;(5)6:1680-1683. https://doi.org/ 10.1016/j.ijggc.2011.08.003
119. Fosbøl PL, Thomsen K, Stenby EH. Review and recommended thermodynamic properties of $FeCO_3$. Corros Eng Sci Technol. 2010;(45)2:115-135. https://doi.org/10.1179/174327808X286437
120. Nesic S, Thevenot N, Crolet JL et al. Electrochemical Properties of Iron Dissolution in the Presence of CO_2 - Basics Revisited. NACE Corros. 1996. Paper No. NACE-96003.
121. Smith SN, Joosten MW. Corrosion of Carbon Steel by H_2S in CO_2 Containing Oilfield Environments. NACE Corrosion. 2006;(3)12.
122. Dugstad A. Fundamental Aspects of CO_2 Metal Loss Corrosion, Part I: Mechanism. NACE Corrosion. 2015;(3):15.
123. Crolet J. Acid Corrosion in Wells (CO_2/H_2S): Metallurgical Aspects. J Petrol Technol. 1983;(35):1553-1558.
124. Tribollet B, Kittel J, Meroufel A et al. Corrosion mechanisms in aqueous solutions containing dissolved H_2S. Part 2: Model of the cathodic reactions on a 316L stainless steel rotating disc electrode. Electrochim Acta. 2014;(124)12:6-51. https://doi.org/10.1016/j.electacta.2013.08.133
125. Bolmer PW. Polarization of Iron in H_2S-NaHS Buffers. Corrosion. 1965;(21)3:69-75. https://doi.org/10.5006/0010-9312-21.3.69
126. Remita E. A kinetic model of CO_2 corrosion in the confined environment of flexible pipe annulus. HAL Id: hal-02475569. 2020
127. Xi Y, Li Y, Yao Y et al. Identification and Analysis of Corrosion Mechanisms for Ground Pipelines with Hanging Rings. Coatings. 2022;(12)1257. https://doi.org/10.3390/coatings12091257
128. Abbas MH. Modelling CO_2 Corrosion of Pipeline Steels. School of Marine Science and Technology, Newcastle University, 2016. http://theses.ncl.ac.uk/jspui/handle/10443/3529. http://hdl.handle.net/10443/3530
129. Obot IB, Solomon MM, Savour A et al. Progress in the development of sour corrosion inhibitors: Past, present and future perspectives. J Ind Eng Chem. 2019;(79):1-18. https://doi.org/10.1016/j.jiec.2019.06.046
130. Sun W, Pugh DV, Smith SN et al. A parametric study of sour corrosion of carbon steel. NACE-Int Corros Conf Ser Expo. 2010. Paper No 10278.
131. Sun W, Nesic S. A mechanistic model of H_2S corrosion of mild steel. NACE-Int Corros Conf Series. 2007;(07655):076551-0765526.
132. Wen AX, Bai P, Luo B. Review of Recent progress in the study of corrosion products of steel in a hydrogen sulfide environment. Corros Sci. 2018;(139):124-140. https://doi.org/10.1016/j.corsci.2018.05.002
133. Umoren SA, Solomon MM, Saji VS. Corrosion inhibitors for sour oilfield environment (H_2S corrosion). Corros Inh Oil Gas Ind. 2020;(2):229-254. https://doi.org/10.1002/9783527822140.ch8
134. Shoesmith DW, Taylor P, Bailey MG. Electrochemical behaviour of iron in Alkaline Sulphide Solutions. Electrochim Acta. 1978;(23):903-916. https://doi.org/10.1016/0013-4686(78)87014-5

135. Jinks JL. The Analysis of Continuous Variation in a Diallel Cross of Nicotiana Rustica Varieties Genetics. 1954;(39)6:767-788. https://doi.org.10.1093/genetics.59.6.767
136. Nešić S. Key issues related to modeling of internal corrosion of oil and gas pipelines - A review. Corros Sci. 2007;(49)12:4308-4338. https://doi.org/10.1016/j.corsci.2007.06.006
137. Zheng S, Li C, Qi Y et al. Mechanism of (Mg, Al, Ca)-oxide inclusion-induced pitting corrosion in 316L stainless steel exposed to sulfur environments containing chloride ion. Corros Sci. 2013;(67):20-31. https://doi.org/10.1016/j.corsci.2012.09.044
138. Rickard D, Morse JW. Acid volatile sulfide (AVS). Marine Chem. 2005;(97):3-4:141-197. https://doi.org/10.1016/j.marchem.2005.08.004
139. Smith SN. Current Understanding of Corrosion Mechanisms Due to H_2S in Oil and Gas Production Environments. NACE Int Corros Conf Expo. 2015. Paper No 5485.
140. Ma H, Cheng X, Li G et al. The influence of hydrogen sulfide on the corrosion of iron under different conditions. Corros Sci. 200;(42)10:1669-1683. https://doi.org/10.1016/50010-938X(00)00003-2
141. Tuttle RN, Co SO. Corrosion in Oil and Gas Production. J Petrol Technol. 1987;(7):756-762. https://doi.org/10.2118/1700-PA
142. Macedo JF, Fioravante IA, Nakazato RZ et al. Corrosion Behavior of API 5L X70 Carbon Steels in Hydrogen Sulfide Environments. Iranian J Mat Sci Eng. 2021;(18)118-127. https://doi.org/10.22068/ijmse.18.1.12
143. Mohtadi-Banab MA, Szpunar JA, Basu R, et al. The mechanism of failure by hydrogen-induced cracking in an acidic environment for API 5L X70 pipeline steel. Int J Hydrogen Ener. 2015;(40)2:1096-1107. https://doi.org/10.1016/j.ijhydene.2014.11.057
144. Wolthers M, Gaast SJ, Rickard D. The structure of disordered mackinawite Amer Mineralog. 2003:88(11-12-Part2):2007-2015. https://doi.org/10.2138/am-2003-11-1245
145. Taylor P, Videla HA. An overview of mechanisms by which sulfate-reducing bacteria influence steel corrosion in marine environments Biofouling: J Bioadhes Biof. 2009;(3):37-47. https://doi.org/10.1080/08927010009386296
146. Zheng S, Zhou C, Chen X et al. Dependence of the abnormal protective property on the corrosion product film formed on H_2S-adjacent API-X52 pipeline steel. Int J Hydrogen Energy. 2014L(17):1-7. https://doi.org/10.1016/j.ijhydene.2014.04.077
147. Santos G, Loh W, Bannwart A et al. An Overview of Heavy Oil Properties and its Recovery and Transportation Methods. Brazil J Chem Eng. 2014;(31)3:571-590. https://doi.org/10.1590/0104-6632.20140313s00001853
148. Bockris JOM, Drazic D. The Kinetics of Deposition and Dissolution of Iron: Effect of Alloying Impurities. Electrochim Acta. 1962;(7)3:293-313. https://doi.org/10.1016/0013-4686(62)87007-8

149. Meyer FH. Corrosion Products of Mild Steel in Hydrogen Sulfide Environments. Corrosion. 1958;(14)2:69-75. https://doi.org/10.5006/0010-9312-14.2.69
150. Smith SN, Pacheco JL. Prediction of corrosion in slightly sour environments. NACE – Int Corros Conf Series. 2002. Paper No 02241.
151. Shoesmith DW, Taylor P, Bailey MG. The Formation of Ferrous Monosulfide Polymorphs during the Corrosion of Iron by Aqueous Hydrogen Sulfide at 21°C. J Electrochem Soc. 1980;(127)5:1007-1015. https://doi.org/10.1149/1.2129808
152. Shoesmith DW. Formation, Transformation and Dissolution of Phases Formed on Surfaces. Whiteshell Nuclear Research Establishment, Pinawa, Man. AECL-6840 OL2197009M https://id.oclc.org/worldcat/entity/E39QH7Jmr7K87qGBjjD6Gkh43F
153. Smith SN, Wright EJ. Prediction of minimum H_2S levels required for slightly sour corrosion. NACE Int Corr Conf Expo. 1994. Paper No 11.
154. Taylor P. The stereochemistry of iron sulfides structural rationale for the crystallization of some metastable phases from aqueous solution. Amer Miner. 1980;(65);1026-1030. https://www.osti.gov/biblio/6679263
155. Baylis JR. Factors other than Dissolved Oxygen Influencing the Corrosion of Iron Pipes. Ind Eng Chem. 1926;(18)4:370-380. https://doi.org/10.1021/ie50196a012
156. Hackerman N, Glenn EE. Corrosion of Steel by Air-Free, Dilute, Weak Acids. J Electrochem Soc. 1953;(100)8:339. https://doi.org/10.1149/1.2781130
157. Dugstad A. Fundamental aspects of CO_2 metal loss corrosion Part I: Mechanism. NACE Int Corro Conf Expo. Paper No 2015-5826.
158. Zhang H, Pang X, Zhou M et al. Applied Surface Science The behavior of pre-corrosion effect on the performance of imidazoline-based inhibitor in 3 wt .% NaCl solution saturated with CO_2. Appl Surf Sci. 2015;(356):63-72. https://doi.org/10.1016/j.apsusc.2015.08.003
159. Liu H, Fu C, Gu T et al. Corrosion behavior of carbon steel in the presence of sulfate-reducing bacteria and iron-oxidizing bacteria cultured in oilfield-produced water. Eval Program Plann. 2015;(9):1-12. https://doi.org/10.1016/j.corsci.2015.08.023
160. Fosbøl P, Stenby E, Thomsen K. Carbon Dioxide Corrosion: Modelling and Experimental Work Applied to Natural Gas Pipelines. 2008 PhD thesis Technical University of Denmark. Pages 1-237. https://backend.orbit.dtu.dk/ws/portalfiles/portal/5464013/Thesis_CO2_Corrosion_Phillip_Loldrup_Fosb_l_87-91435-89-7_DTU_2008.pdf
161. Kucharski M, Stubina N M, Toguri JM. Viscosity measurements of molten Fe-O-SiO_2, Fe-O-CaO-SiO_2, and Fe-O-MgO-SiO_2 slags. Canad Metallur Quart. 1989;(28):17-11. https://doi.org/10.1179/cmq.1989.28.1.7
162. Preis W, Gamsjäger H. Critical evaluation of solubility data: Enthalpy of formation of siderite. Phys Chem Chem Phys. 2002;(4)16:4014-4019. https://doi.org/10.1039/b203626f

163. Sel O, Radha A V, Dideriksen K et al. Amorphous iron (II) carbonate: Crystallization energetics and comparison to other carbonate minerals related to CO_2 sequestration. Geochim Cosmochim Acta. 2012;(87):61-68. https://doi.org/10.1016/j.gca.2012.03.011
164. Ramanarayanan TA, Smith SN. Corrosion of iron in gaseous environments and in gas-saturated aqueous environments. Corrosion. 1990;(46)1:66-74. https://doi.org/10.5006/1.3585068
165. Rivera-Grau LM, Gonzalez-Rodriguez JG, Martinez L. Effect of Hydroxyethil imidazoline and Ag Nanoparticles on the CO_2 Corrosion of Carbon Steel. Int J Electrochem Sci. 2016;(11):80-94. https://doi.org/10.1016/S1452-3981(23)15828-7
166. Porcayo-CJ, Martinez LM, Canto J et al. Imidazoline Derivatives Based on Coffee Oil as CO_2 Corrosion Inhibitor. Int J Electrochem Sci. 2015;(10)4:3160-3176. https://doi.org/10.1016/S1452-3981(23)06528-8
167. Hinds G, Cooling P, Turnbull A. Testing of inhibitors for under-deposit corrosion in sour conditions Testing of inhibitors for under-deposit corrosion in sour conditions. Eurocorr Conf. 2009;1-9. https://www.researchgate.net/publication/273755924
168. Zhang Y, Pang X, Qu S et al. The relationship between fracture toughness of CO_2 corrosion scale and corrosion rate of X65 pipeline steel under supercritical CO_2 condition. Int J Green Gas Cont. 2011;(5)6:1643-1650. https://doi.org/10.1016/j.ijggc.2011.09.011
169. Cui ZD, Wu SL, Zhu SL. Study on corrosion properties of pipelines in simulated produced water saturated with supercritical CO_2. Appl Surf Sci. 2006;(252)6:2368-2374. https://doi.org/10.1016/j.apsusc.2005.04.008
170. Ekeocha CI, Onyeachu BI, Etim IN et al. Review of forms of corrosion and mitigation techniques. A visual guide. African Sci Rep. 2023;(2)117:1-22. https://doi.org/10.46481/asr.2023.2.3.117